JCI The Journal of Clinical Investigation

The growth factor midkine regulates the renin-angiotensin system in mice

Akinori Hobo, … , Seiichi Matsuo, Kenji Kadomatsu

J Clin Invest. 2009;119(6):1616-1625. https://doi.org/10.1172/JCI37249.

Research Article **Nephrology**

The renin-angiotensin system plays a pivotal role in regulating blood pressure and is involved in the pathogenesis of kidney disorders and other diseases. Here, we report that the growth factor midkine is what we believe to be a novel regulator of the renin-angiotensin system. The hypertension induced in mice by 5/6 nephrectomy was accompanied by renal damage and elevated plasma angiotensin II levels and was ameliorated by an angiotensin-converting enzyme (ACE) inhibitor and an angiotensin receptor blocker. Notably, ACE activity in the lung, midkine expression in the lung, and midkine levels in the plasma were all increased after 5/6 nephrectomy. Exposure to midkine protein enhanced ACE expression in primary cultured human lung microvascular endothelial cells. Furthermore, hypertension was not induced and renal damage was less severe in midkine-deficient mice. Supplemental administration of midkine protein to midkine-deficient mice restored ACE expression in the lung and hypertension after 5/6 nephrectomy. Oxidative stress might be involved in midkine expression, since expression of NADH/NADPH oxidase–1, –2, and –4 was induced in the lung after 5/6 nephrectomy. Indeed, the antioxidative reagent tempol reduced midkine expression and plasma angiotensin II levels and consequently ameliorated hypertension. These results suggest that midkine regulates the renin-angiotensin system and mediates the kidney-lung interaction after 5/6 nephrectomy.

The growth factor midkine regulates the renin-angiotensin system in mice

Akinori Hobo,[1,2] Yukio Yuzawa,[2] Tomoki Kosugi,[2] Noritoshi Kato,[1,2] Naoto Asai,[2] Waichi Sato,[2] Shoichi Maruyama,[2] Yasuhiko Ito,[2] Hiroyuki Kobori,[3] Shinya Ikematsu,[4] Akira Nishiyama,[5] Seiichi Matsuo,[2] and Kenji Kadomatsu[1]

[1]Department of Biochemistry and [2]Department of Nephrology, Nagoya University Graduate School of Medicine, Nagoya, Japan.
[3]Department of Physiology and Hypertension & Renal Center of Excellence, Tulane University Health Sciences Center, New Orleans, Louisiana, USA.
[4]Department of Bioresources Engineering, Okinawa National College of Technology, Okinawa, Japan.
[5]Department of Pharmacology and Hypertension & Kidney Disease Research Center, Kagawa University Medical School, Kagawa, Japan.

The renin-angiotensin system plays a pivotal role in regulating blood pressure and is involved in the pathogenesis of kidney disorders and other diseases. Here, we report that the growth factor midkine is what we believe to be a novel regulator of the renin-angiotensin system. The hypertension induced in mice by 5/6 nephrectomy was accompanied by renal damage and elevated plasma angiotensin II levels and was ameliorated by an angiotensin-converting enzyme (ACE) inhibitor and an angiotensin receptor blocker. Notably, ACE activity in the lung, midkine expression in the lung, and midkine levels in the plasma were all increased after 5/6 nephrectomy. Exposure to midkine protein enhanced ACE expression in primary cultured human lung microvascular endothelial cells. Furthermore, hypertension was not induced and renal damage was less severe in midkine-deficient mice. Supplemental administration of midkine protein to midkine-deficient mice restored ACE expression in the lung and hypertension after 5/6 nephrectomy. Oxidative stress might be involved in midkine expression, since expression of NADH/NADPH oxidase–1, –2, and –4 was induced in the lung after 5/6 nephrectomy. Indeed, the antioxidative reagent tempol reduced midkine expression and plasma angiotensin II levels and consequently ameliorated hypertension. These results suggest that midkine regulates the renin-angiotensin system and mediates the kidney-lung interaction after 5/6 nephrectomy.

Introduction

The renin-angiotensin system (RAS) is a hormonal cascade that functions in the homeostatic control of arterial pressure, tissue perfusion, and extracellular volume. Dysregulation of the RAS results in the pathogenesis of many diseases, including cardiovascular and renal disorders (1–3). The RAS is initiated by the regulated secretion of renin, which catalyzes the hydrolysis of Ang I from the N terminus of angiotensinogen. Ang I is in turn hydrolyzed by angiotensin-converting enzyme (ACE) to form Ang II, the primary active product of the RAS (4, 5). ACE is a zinc metallopeptidase widely distributed on the cell membrane of endothelial and epithelial cells (6). Ang II induces vasoconstriction and aldosterone release, leading to upregulation of blood pressure. It also exerts its vasoconstrictor effect on both the afferent and efferent arterioles, which may contribute to the onset and progression of chronic renal damage. Ang II may also directly contribute to the acceleration of renal damage by sustaining cell growth, inflammation, and fibrosis (7).

The growth factor midkine (MK; gene symbol, *MDK*) is implicated in cancer progression, neuronal survival and differentiation, and inflammation (8). MK is involved in the pathogeneses of tubulointerstitial damage induced by renal reperfusion and glomerular sclerosis associated with diabetes mellitus (9, 10). The finding of a recent report that angiotensinogen and renin expression was significantly elevated in the aorta of *Mdk*$^{-/-}$ mice while ACE expression was significantly suppressed is of particular interest (11). However, *Mdk*$^{-/-}$ mice develop normally (8), and there has been no report of systemic disturbance or organ disorders of *Mdk*$^{-/-}$ mice. Therefore, the biological meaning of changes in the RAS molecules in the aorta of *Mdk*$^{-/-}$ mice has remained obscure.

It is widely accepted that the RAS is involved in the pathogenesis of chronic kidney disease (CKD), and inhibitors of the RAS are the first choice of therapy for CKD (12–14). To investigate the molecular mechanisms regulating the RAS in CKD, we employed 5/6 nephrectomy in this study. 5/6 nephrectomized mice are a popular and useful model of CKD, since the remnant kidney model of progressive renal injury is characterized by systemic hypertension and glomerular hyperfiltration, the latter eventually causing glomerular sclerosis (15, 16). CKD accompanies multiple organ failure, the pathogenesis of which involves inter-organ cross-talk (17, 18). In this context, it is noteworthy that MK expression was induced in the lung by 5/6 nephrectomy, leading to elevation of ACE activity and plasma Ang II levels and subsequent hypertension in the present study. Our data therefore suggest that MK is a candidate mediator of inter-organ cross-talk in CKD.

Results

MK is involved in RAS activation induced by 5/6 nephrectomy. Systolic and mean blood pressure were comparable in untreated *Mdk*$^{+/+}$ and *Mdk*$^{-/-}$ mice (Figure 1, A and B). However, we found that 5/6 nephrectomy strikingly increased blood pressure in *Mdk*$^{+/+}$ mice but not in *Mdk*$^{-/-}$ mice (Figure 1, A and B). The systolic and mean blood pressure of *Mdk*$^{+/+}$ mice strikingly increased after 2 weeks, but *Mdk*$^{-/-}$ mice showed almost normal blood pressure, i.e., no

Conflict of interest: The authors have declared that no conflict interest exists.

Nonstandard abbreviations used: ACE, angiotensin-converting enzyme; BIS, bisindolylmaleimide I; CKD, chronic kidney disease; HMVEC-L, human lung microvascular endothelial cell(s); MK, midkine; Nox, NADPH oxidase; PTN, pleiotrophin; RAS, renin-angiotensin system; rh-MK, recombinant human MK.

Citation for this article: *J. Clin. Invest.* **119**:1616–1625 (2009). doi:10.1172/JCI37249.

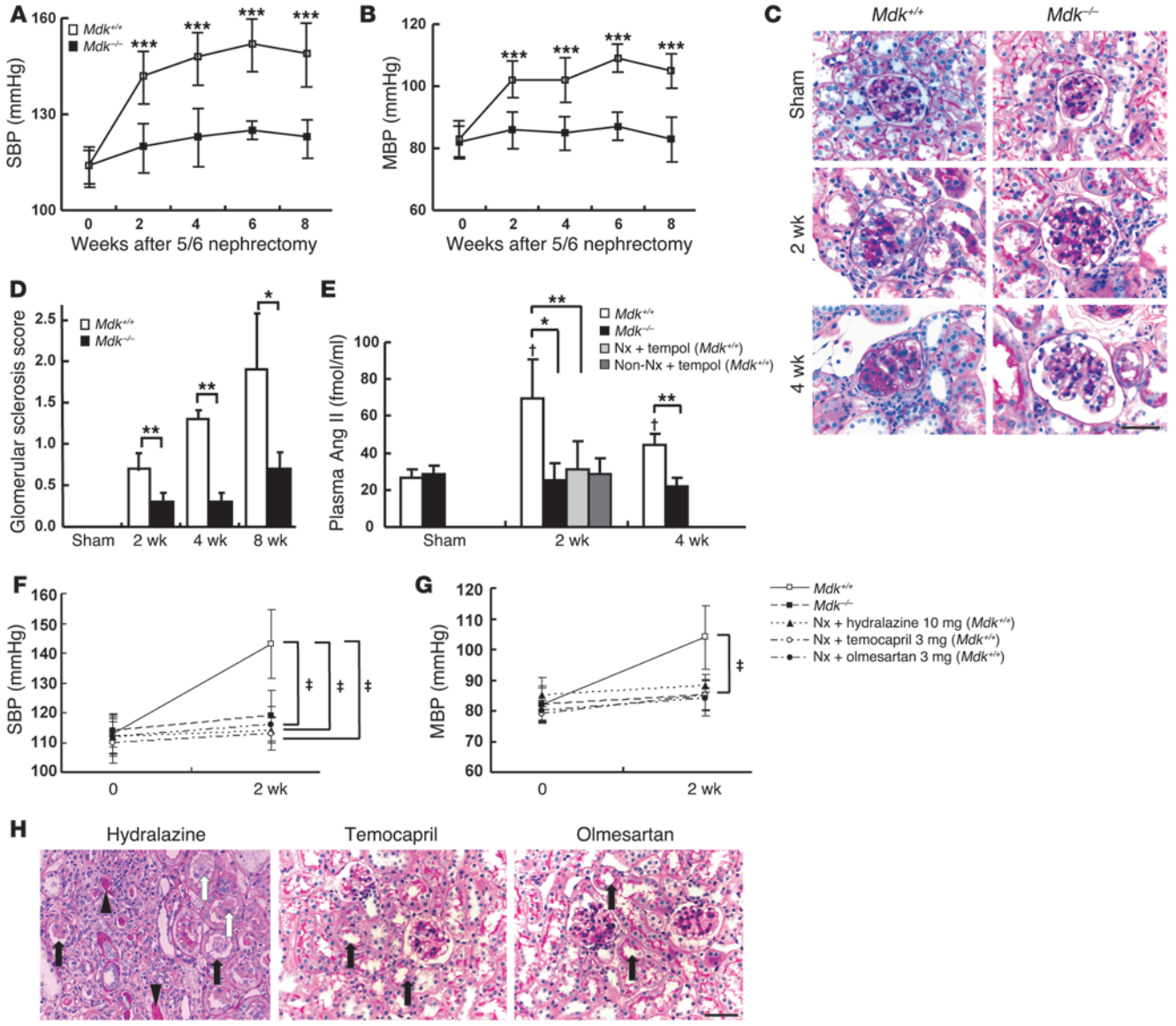

Figure 1

5/6 nephrectomy induces hypertension and renal damage via the RAS. (**A** and **B**) Blood pressure was measured at 0, 2, 4, 6, and 8 weeks after 5/6 nephrectomy. Systolic blood pressure (SBP) (**A**) and mean blood pressure (MBP) (**B**) were measured by the tail-cuff method. The mean and SD are represented by squares and bars, respectively, at each time point ($Mdk^{+/+}$: 0 weeks, $n = 40$; 2 weeks, $n = 34$; 4 weeks, $n = 19$; 8 weeks, $n = 8$; $Mdk^{-/-}$: 0 weeks, $n = 26$; 2 weeks, $n = 23$; 4 weeks, $n = 13$; 8 weeks, $n = 4$). ***$P < 0.001$ versus $Mdk^{-/-}$ mice. (**C**) Representative glomerular histology shown by PAS staining. Scale bar: 50 μm. (**D**) Semiquantitative analysis of the glomerular sclerosis score. Data are shown as mean and SD ($Mdk^{+/+}$: 2 weeks, $n = 5$; 4 weeks, $n = 4$; 8 weeks, $n = 4$; $Mdk^{-/-}$: 2 weeks, $n = 4$; 4 weeks, $n = 3$; 8 weeks, $n = 3$). (**E**) Plasma Ang II concentration after 5/6 nephrectomy ($Mdk^{+/+}$: sham, $n = 6$; 2 weeks, $n = 6$; 4 weeks, $n = 8$; $Mdk^{-/-}$: sham, $n = 6$; 2 weeks, $n = 7$; 4 weeks, $n = 5$). *$P < 0.05$, **$P < 0.01$; †$P < 0.01$ versus sham $Mdk^{+/+}$. Nx, nephrectomy. (**F** and **G**) Effects of hydralazine, temocapril, and olmesartan on blood pressure. SBP (**F**) and MBP (**G**) were measured by the tail-cuff method ($n = 3$). ‡$P < 0.01$ versus $Mdk^{+/+}$ mice. (**H**) Representative histology after treatment with hydralazine, temocapril, and olmesartan. The kidney specimens were stained with PAS. Tubular dilatation (black arrows), tubular cast formation (arrowheads), and tubular degeneration (white arrows) are indicated. Scale bar: 50 μm.

significant increase (systolic blood pressure, 143 ± 11.6 mmHg in $Mdk^{+/+}$ mice vs. 119 ± 8.6 mmHg in $Mdk^{-/-}$ mice; mean blood pressure, 104 ± 10.3 mmHg vs. 85 ± 6.7 mmHg). Consequently, systolic and mean blood pressures were significantly higher in $Mdk^{+/+}$ than in $Mdk^{-/-}$ mice from 2 to 8 weeks (Figure 1, A and B).

5/6 nephrectomy caused not only hypertension but also progressive renal failure. Blood urea nitrogen and serum creatinine levels gradually increased, and both parameters were significantly higher in $Mdk^{+/+}$ mice at 2 and 4 weeks after renal ablation (Table 1). $Mdk^{+/+}$ mice also exhibited more severe glomerular sclerosis, which is characterized by a marked deposition of extracellular matrix in the glomeruli and which occurred as early as 2 weeks after renal ablation (Figure 1C). Semiquantitative analysis of the glomerular sclerosis scores revealed significant differences between $Mdk^{+/+}$

Table 1
Body weight, blood urea nitrogen, serum creatinine, and left kidney weight after 5/6 nephrectomy

	BW (g)	BUN (mg/dl)	Cre (mg/dl)	Left kidney wt (mg)
Before nephrectomy				
Mdk$^{+/+}$	22.2 ± 2.1	21.2 ± 3.7	0.06 ± 0.02	–
Mdk$^{-/-}$	21.3 ± 1.3	19.7 ± 1.4	0.04 ± 0.02	–
Hydralazine, 10 mg/kg/d	23.1 ± 0.6	ND	ND	–
Temocapril, 3 mg/kg/d	22.0 ± 2.0	ND	ND	–
Olmesartan, 3 mg/kg/d	24.5 ± 0.5	ND	ND	–
Tempol, 3 mmol/l	22.7 ± 1.7	ND	ND	–
2 weeks after nephrectomy				
Mdk$^{+/+}$	19.7 ± 2.2	57.1 ± 9.7	0.65 ± 0.11	104.8 ± 9.6
Mdk$^{-/-}$	18.8 ± 1.5	39.5 ± 7.2^{A}	0.39 ± 0.08^{A}	104.3 ± 15.1
Hydralazine, 10 mg/kg/d	18.7 ± 0.7	63.3 ± 7.6	0.53 ± 0.12	ND
Temocapril, 3 mg/kg/d	19.7 ± 2.7	30.3 ± 2.9^{A}	0.21 ± 0.04^{A}	ND
Olmesartan, 3 mg/kg/d	21.3 ± 0.7	36.0 ± 1.0^{B}	0.21 ± 0.01^{A}	ND
Tempol, 3 mmol/l	21.4 ± 1.6	41.2 ± 3.9^{B}	0.25 ± 0.04^{A}	ND
4 weeks after nephrectomy				
Mdk$^{+/+}$	20.9 ± 1.8	66.1 ± 8.7	0.77 ± 0.13	130.0 ± 21.4
Mdk$^{-/-}$	20.6 ± 1.7	46.4 ± 4.8^{A}	0.44 ± 0.15^{B}	130.3 ± 10.7
8 weeks after nephrectomy				
Mdk$^{+/+}$	22.5 ± 1.9	71.9 ± 14.6	1.56 ± 0.34	118.5 ± 14.9
Mdk$^{-/-}$	21.2 ± 2.3	62.9 ± 12.9	1.18 ± 0.29	128.5 ± 6.0

Values are mean ± SD. BUN, blood urea nitrogen; Cre, serum creatinine. ND, no data. Hydralazine, temocapril, olmesartan, and tempol were administered to *Mdk*$^{+/+}$ mice at the indicated doses. $^{A}P < 0.001$ versus *Mdk*$^{+/+}$. $^{B}P < 0.01$ versus *Mdk*$^{+/+}$.

and *Mdk*$^{-/-}$ mice (Figure 1D). In addition, the tubulointerstitial damage was worse in *Mdk*$^{+/+}$ mice (Supplemental Figure 1; supplemental material available online with this article; doi:10.1172/JCI37249DS1). Thus, tubular dilatation, cast formation in the tubular lumen, and tubular epithelial degeneration became apparent at 2 weeks after renal ablation and were more severe in *Mdk*$^{+/+}$ mice (Supplemental Figure 1, A–H). Interstitial fibrosis, as evidenced by collagen deposition revealed by Masson's trichrome staining, was exhibited at 4 weeks and then more diffusely at 8 weeks, and the stained area became expanded in *Mdk*$^{+/+}$ mice (Supplemental Figure 1, I–P). These data collectively indicate that renal damage was more severe in *Mdk*$^{+/+}$ mice than in *Mdk*$^{-/-}$ mice.

These symptoms of hypertension and renal damage were attributable to the RAS, as (a) the hypertension was accompanied by elevated plasma Ang II concentration (Figure 1E); and (b) the ACE inhibitor temocapril and the angiotensin receptor blocker olmesartan reduced both blood pressure and renal tubulointerstitial damage, but the vasodilator hydralazine only ameliorated hypertension (Figure 1, F–H). Abnormal elevation of blood urea nitrogen and serum creatinine was ameliorated by administration of temocapril and olmesartan, but not hydralazine (Table 1). It is therefore conceivable that the RAS contributed to both hypertension and renal damage.

ACE levels are increased in the lung after 5/6 nephrectomy. Expression of the intrarenal angiotensinogen and renin was suppressed and ACE expression was unchanged in *Mdk*$^{+/+}$ mice, which was consistent with previous findings after 5/6 nephrectomy of rats (19, 20) (Supplemental Figure 2, A–C). In contrast to the kidney, the lung showed significant increases in ACE expression and its activity 2 and 4 weeks after renal ablation (Figure 2, A–E). ACE protein expression was localized to the pulmonary vascular endothelial cells and alveolar-capillary endothelial cells, consistent with a previous report (Figure 2D) (21).

Other organs that play major functions in the RAS were also examined for their expression of RAS components. Angiotensinogen mRNA expression was induced in the liver after 5/6 nephrectomy, but the expression level was not significantly different in *Mdk*$^{+/+}$ and *Mdk*$^{-/-}$ mice (Supplemental Figure 3A). There was no difference in angiotensinogen protein levels between the two genotypes (Supplemental Figure 3, B and C), and renin mRNA expression was not detected in the liver (data not shown). Expression of ACE protein and MK protein was also not detected in the liver (Supplemental Figure 3, D and E). In the brain, mRNA expression of angiotensinogen and ACE did not change after 5/6 nephrectomy (Supplemental Figure 4, A and B), and the renin mRNA expression was undetectable (data not shown). ACE protein was also not detected in the brain (Supplemental Figure 4C). Furthermore, the mRNA expression of angiotensinogen, renin, and ACE did not change in the heart (Supplemental Figure 5). Therefore, it is most likely that the hypertension observed after 5/6 nephrectomy was due to activation of the lung ACE.

MK levels are increased in the lung, kidney, and plasma after 5/6 nephrectomy. MK expression was increased in the lung in association with an elevation in ACE expression (Figure 3, A–C). MK protein was localized to the endothelium of microvessels of the lung, as revealed by the use of thrombomodulin as a marker of the vascular endothelium (Figure 3D). MK expression was detected in alveolar-capillary endothelial cells but not in bronchial epithelial cells (Figure 3D).

Histological evidence of lung damage, i.e., due to edema and degeneration of alveolar cells, was not observed after 5/6 nephrectomy in the *Mdk*$^{+/+}$ and *Mdk*$^{-/-}$ mice (Supplemental Figure 6A). Increases in macrophage and neutrophil infiltration into the lung were also not observed after 5/6 nephrectomy in the two genotypes (Supplemental Figure 6, B–E). These results indicated that the increase in MK expression in the lung after 5/6 nephrectomy was not due to leukocytes.

MK expression was also significantly elevated in the kidney at both the protein and mRNA levels 2 and 4 weeks after renal ablation (Supplemental Figure 7, A–C). Immunohistochemical analysis revealed that MK protein was mainly localized in the tubular epithelium (Supplemental Figure 8A). This result is consistent with previous reports in which MK was expressed in the kidney after ischemia/reperfusion injury and its associated massive leukocyte infiltration (22). We also detected a substantial increase in macrophage infiltration into the kidney after 5/6 nephrectomy, and this increase was significantly higher in *Mdk*$^{+/+}$ mice than *Mdk*$^{-/-}$ mice (Supplemental Figure 8, B and C). It is known that MK is expressed by activated macrophages (23, 24). Thus, it is conceivable that the increase in MK expression in the kidney after 5/6 nephrectomy was due to enhanced expression in both the tubular epithelium and infiltrating macrophages.

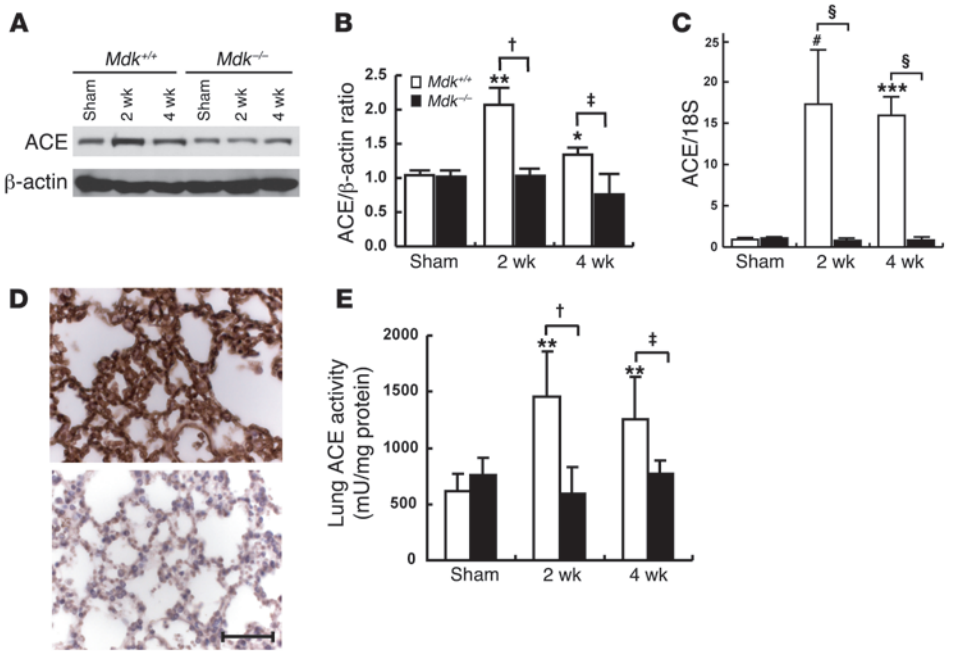

Figure 2

ACE expression in the lung after 5/6 nephrectomy. (**A**) ACE protein was determined by Western blotting, and a representative result is shown. The lung tissues were obtained at the indicated time points. (**B**) Quantitative analysis of ACE protein expression using densitometry. Data are presented as mean and SD ($n = 3$). $^{\dagger}P < 0.01$; $^{\ddagger}P < 0.05$; $^{*}P < 0.05$ and $^{**}P < 0.01$ versus sham *Mdk*$^{+/+}$. (**C**) ACE mRNA was determined by real-time PCR and normalized to 18S mRNA. Data are presented as mean and SD (*Mdk*$^{+/+}$: sham, $n = 5$; 2 weeks, $n = 5$; 4 weeks, $n = 3$; *Mdk*$^{-/-}$: sham, $n = 3$; 2 weeks, $n = 3$; 4 weeks, $n = 3$). $^{\S}P < 0.0001$; $^{***}P < 0.001$ and $^{\#}P < 0.0001$ versus sham *Mdk*$^{+/+}$. (**D**) Immunohistochemical staining of lungs with mouse anti-ACE monoclonal antibody at 2 weeks. Upper panel: The first antibody used was anti–mouse ACE monoclonal antibody. Lower panel: Isotype-matched IgG was used as the first antibody. Scale bar: 50 μm. (**E**) ACE activity was determined by the ACE activity assay, as described in Methods. Data are presented as mean and SD (*Mdk*$^{+/+}$: sham, $n = 5$; 2 weeks, $n = 5$; 4 weeks, $n = 5$; *Mdk*$^{-/-}$: sham, $n = 5$; 2 weeks, $n = 5$; 4 weeks, $n = 4$). $^{\dagger}P < 0.01$; $^{\ddagger}P < 0.05$; $^{**}P < 0.01$ versus sham *Mdk*$^{+/+}$.

Since MK is a secreted protein, and its expression was induced by 5/6 nephrectomy in the kidney and lung (Figure 3, A–C, and Supplemental Figure 7, A–C), we next examined plasma MK levels. As shown in Figure 3, E and F, plasma MK levels were indeed increased 2 weeks after 5/6 nephrectomy.

Exogenous MK induces ACE expression. If MK is required for ACE expression in the lung and hypertension, supplementary administration of MK might also affect these symptoms. To clarify this issue, we administered exogenous MK continuously through an osmotic pump into *Mdk*$^{-/-}$ mice after 5/6 nephrectomy. This administration was found to restore hypertension and ACE expression in the lung (Figure 4, A–C). We also administered pleiotrophin (PTN; also called HB-GAM), which shows 50% homology with MK (8), to *Mdk*$^{-/-}$ mice after 5/6 nephrectomy. However, exogenous PTN neither induced hypertension nor increased ACE expression in the lung (Figure 4, A, D, and E). These data support the specificity of MK with respect to its involvement in ACE expression and blood pressure regulation.

Furthermore, exogenous MK protein on primary cultured human lung microvascular endothelial cells (HMVEC-L) significantly enhanced ACE expression, suggesting that ACE is one of the targets of MK in the lung (Figure 5, A and B). When Ang I was added to the culture medium of the lung endothelial cells treated with MK and heparin for 36 hours, Ang I was converted to Ang II in a time-dependent manner, while cells treated with heparin alone did not show such a conversion (Figure 5C). These results suggest that MK is a potent inducer of Ang II through upregulation of ACE expression in lung endothelial cells.

Along with the increase in ACE expression, phosphorylation levels of PKC were also increased in primary cultured HMVEC-L after exposure to exogenous MK (Figure 5, D and E). This result suggests that MK upregulates ACE expression through activation of PKC. This idea was further supported by three lines of evidence. First, bisindolylmaleimide I (BIS), a PKC-specific inhibitor, blocked the MK-mediated increase in ACE expression (Figure 5, A and B). Second, PKC phosphorylation was significantly increased in the lungs of *Mdk*$^{+/+}$ but not *Mdk*$^{-/-}$ mice after 5/6 nephrectomy (Figure 5F). Third, consistent with previous reports (25), the increase in ACE expression in primary cultured HMVEC-L was also induced by PMA, a PKC activator, and was blocked by BIS (Supplemental Figure 9).

Oxidant stress induces MK expression in the lung after 5/6 nephrectomy. Finally, the mechanism of MK induction in the lung by 5/6 nephrectomy was investigated. The NADPH oxidases (Nox's) are superoxide-generating enzymes that release superoxide by electron transfer from NADPH to oxygen. Increased production of ROS has been implicated in various pathologies, including hypertension, atherosclerosis, diabetes, and CKD (26, 27). In the present study, Nox1, -2, and -4 mRNA expression in the lungs of *Mdk*$^{+/+}$ mice was found to be significantly increased at 2 and 4 weeks after renal ablation compared with the levels in the sham-operated animals, suggesting that oxidant stress was generated in the lung; in contrast, the expression of Nox1, -2, and -4 mRNA was unchanged in the *Mdk*$^{-/-}$ mice (Figure 6A). A cell membrane–permeable radical scavenger, 4-hydroxy-2,2,6,6-tetramethylpiperidine-*N*-oxyl (tempol), reduced MK expression to normal levels in the lung (Figure 6B); plasma Ang II levels (Figure 1E) and blood pressure (Figure 6C) were also reduced. Tempol also ameliorated glomerular sclerosis and tubulointerstitial damage (Figure 6D) and improved renal function, i.e., significantly reduced blood urea nitrogen and serum creatinine levels (Table 1). These results suggest that MK expression was induced by oxidative stress in the lung after 5/6 nephrectomy. Tempol also reduced MK expression in the kidney (Supplemental Figure 7, D and E).

Discussion

Our study demonstrated that *Mdk*$^{-/-}$ mice had almost normal blood pressure after 5/6 nephrectomy, while wild-type mice showed

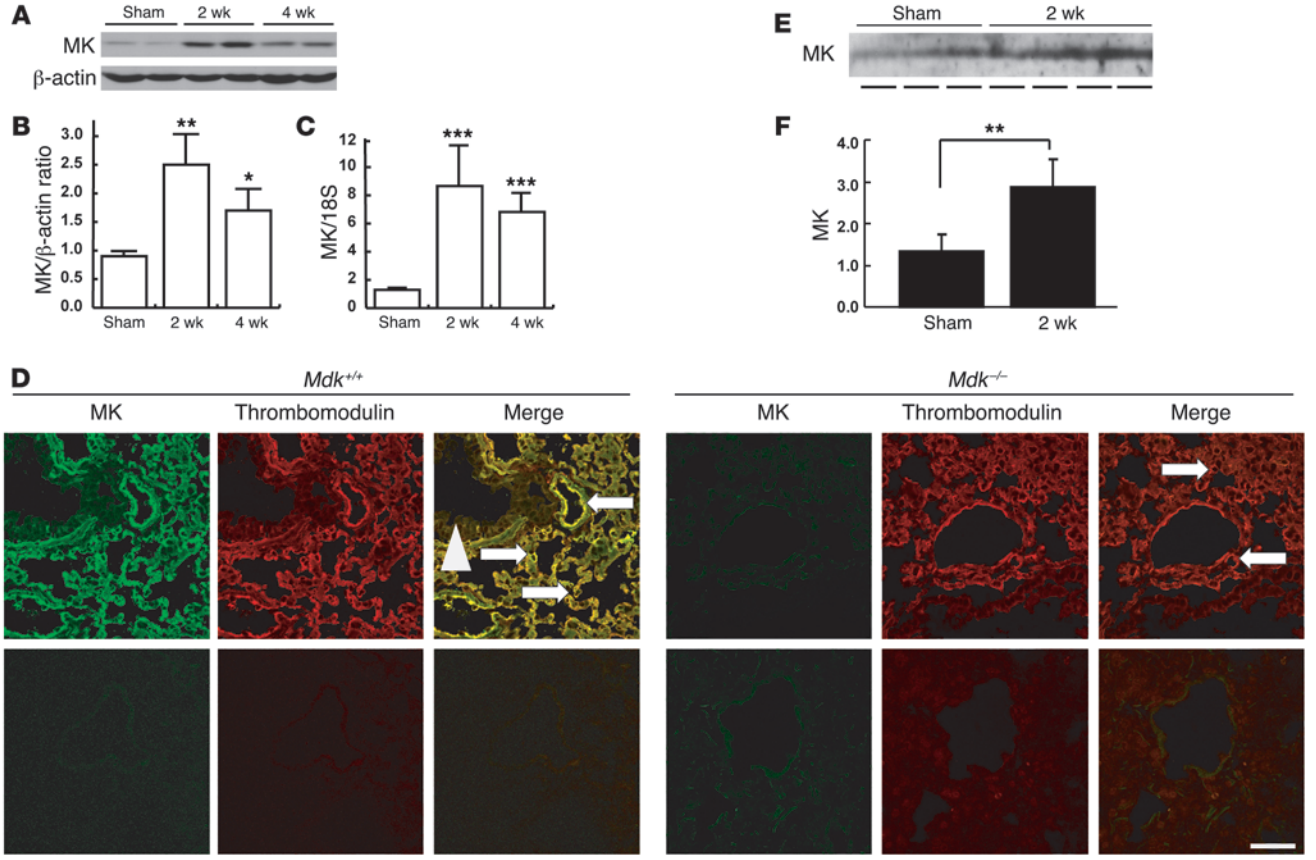

Figure 3

MK expression in the lung and plasma after 5/6 nephrectomy. (**A**) Representative data from Western blotting for MK expression in the lung. (**B**) The intensity of MK bands on Western blotting was normalized to that of β-actin. Data are presented as mean and SD ($n = 4$). $^{*}P < 0.05$ and $^{**}P < 0.01$ versus sham. (**C**) MK mRNA expression in the lung was determined by real-time PCR and normalized to 18S mRNA. Data are presented as mean and SD (sham, $n = 5$; 2 weeks, $n = 5$; 4 weeks, $n = 3$). $^{***}P < 0.001$ versus sham. (**D**) Immunofluorescence staining of MK and thrombomodulin expression in the lung 2 weeks after 5/6 nephrectomy. Lower panels show negative controls using isotype-matched IgG as the first antibody. Arrowhead, bronchial epithelial cells; white arrows, alveolar-capillary endothelial cells. Scale bar: 50 μm. (**E**) Representative data from Western blotting for MK expression in plasma are shown. Lines under the blot indicate individual samples. (**F**) Western blot data for plasma MK were quantified using densitometry and are presented as mean and SD (sham, $n = 4$; 2 weeks, $n = 5$). $^{**}P < 0.01$.

marked hypertension. This hypertension was ameliorated by RAS-related inhibitors and indeed was accompanied by elevated plasma Ang II levels. Surprisingly, ACE activity was enhanced in the lung, whereas RAS components were not activated in other organs. Plasma MK levels and MK expression in the lung and kidney were elevated. Supplementary MK administration to *Mdk*$^{-/-}$ mice restored lung ACE expression and hypertension. MK also induced ACE expression and consequently conversion from Ang I to Ang II in primary cultured lung microvascular endothelial cells. We therefore concluded that MK-mediated ACE induction in the lung is critical for hypertension induced by 5/6 nephrectomy (Figure 7).

Inter-organ interactions involving the kidney have recently been highlighted. Regarding factors affecting lung function after acute kidney injury, several cytokines, including IL-6, IL-1β, and TNF-α, have been suggested as candidates (28, 29). Such results contribute to our understanding of the high mortality associated with pulmonary complications following acute kidney injury. CKD has also been linked with damage in other organs, especially with cardiovascular damage (so-called cardiorenal syndrome) (30). It is particularly interesting that RAS components are increased in the heart and brain of subtotally nephrectomized rats (20, 31) and that Ang II amounts are increased in the isolated perfused hind limbs of uremic rats (32). Inhibitors of the RAS, e.g., angiotensin receptor blockers and ACE inhibitors, are indeed the first choice of therapy for CKD (33). Our results clearly show that the lung is a promising target in the cross-talk between the kidney and other organs and suggest that MK is a candidate mediator for pulmonary and other organ complications associated with CKD.

Regarding the cross-talk between the kidney and lung in 5/6 nephrectomy, our study has also provided an insight into the underlying mechanism. We found that Nox1, -2, and -4 were induced in the lung and that tempol reduced MK and plasma Ang II levels. Nox mediates the initial reaction of 3 successive reduction products of molecular oxygen, i.e., superoxide ($O_2^{\bullet -}$), hydrogen peroxide (H_2O_2), and hydroxyl radical ($OH^{\bullet}$). Since tempol is a membrane-permeable and metal-independent superoxide dismutase mimetic that is specific for superoxide anion ($O_2^{\bullet -}$) (34, 35), tempol may target ROS initiated by Nox in the lung. To the best of our knowledge, this is the first study to show that 5/6 nephrectomy induces oxidative stress in the lung. We have previously reported that oxidative

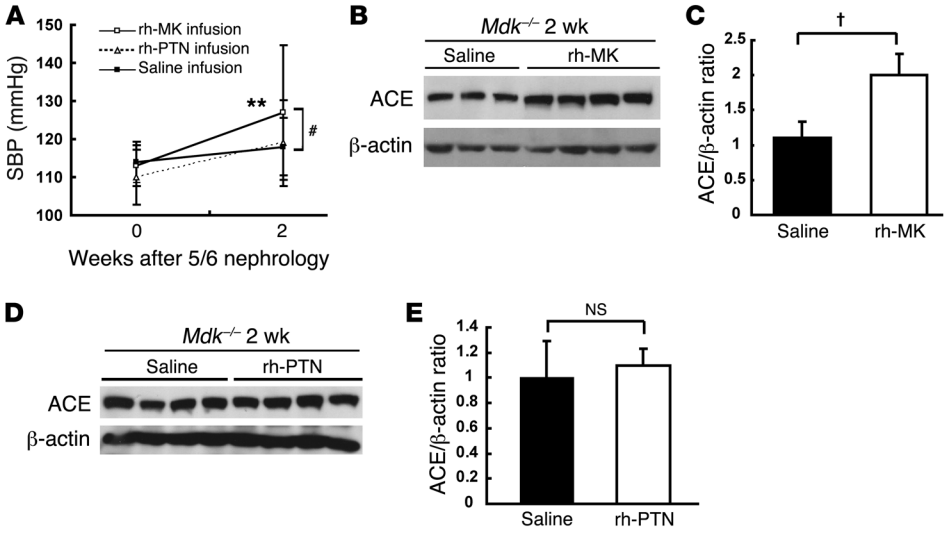

Figure 4
Effects of exogenous MK and PTN in *Mdk*$^{-/-}$ mice on blood pressure and ACE expression in the lung. (**A**) SBP was measured by the tail-cuff method at 0 and 2 weeks after 5/6 nephrectomy (n = 5). $^{**}P < 0.01$ versus untreated *Mdk*$^{-/-}$ mice (0 weeks); $^{\#}P < 0.01$, rh-MK versus saline. rh-PTN, recombinant human PTN. (**B**) ACE expression in the lung of *Mdk*$^{-/-}$ mice treated with MK and saline. Western blot data are shown. (**C**) The data in **B** were quantified using densitometry and are presented as mean and SD. $^{\dagger}P < 0.01$. (**D**) ACE expression in the lung of *Mdk*$^{-/-}$ mice treated with rh-PTN and saline. Western blot data are shown. (**E**) The data in **D** were quantified using densitometry and are presented as mean and SD.

stress induces MK expression (10, 22). Therefore, it is conceivable that Nox-mediated ROS production leads to an induction of MK expression in the lung (Figure 7). As ROS have very short half-lives (36), it is not likely that the ROS themselves travel between the kidney and lung. Furthermore, it is widely accepted that Ang II induces Nox expression (37). Based on this background data, we speculate that the following molecular circuit is established after circulating MK induces ACE expression in the lung: Ang II induces Nox expression, which in turn initiates ROS production and subsequently MK and ACE expression (Figure 7).

RAS-related inhibitors, but not hydralazine, ameliorated renal damage in the present study. It has also been reported that systemically administered Ang II worsens renal function (38–40). Therefore, the RAS might play at least a partial role in renal damage. In

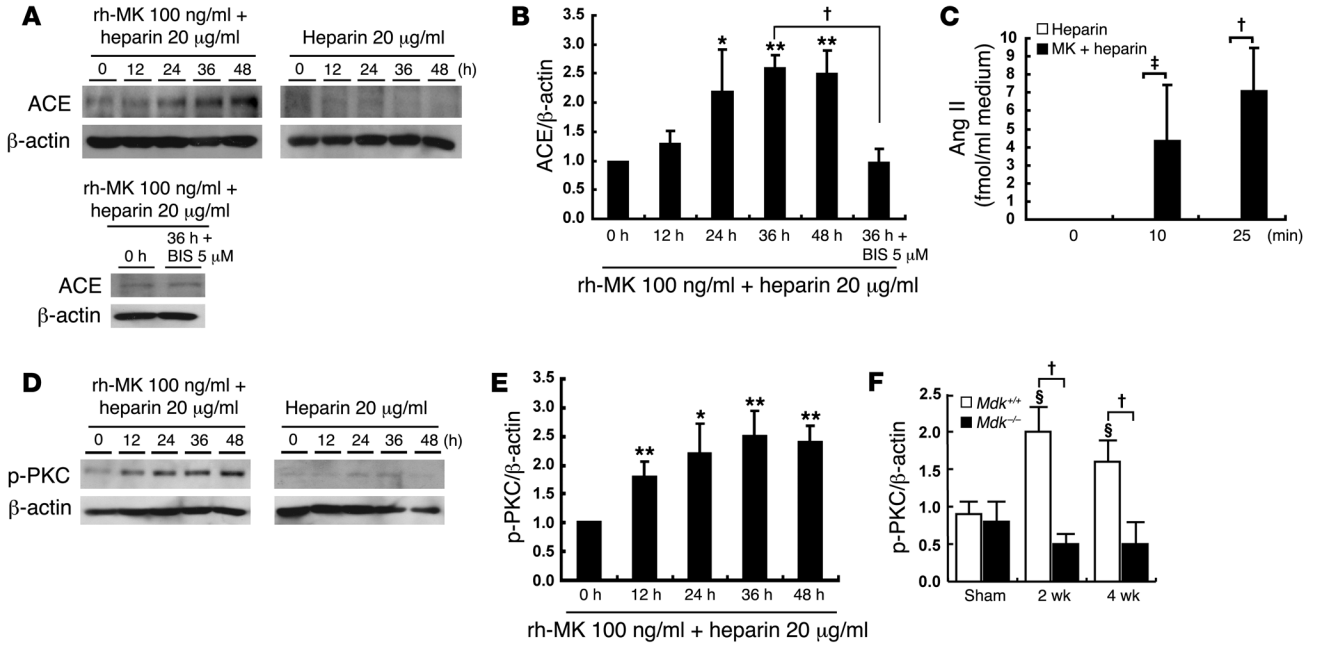

Figure 5
Mechanism of ACE induction by MK in HMVEC-L. (**A**) ACE expression in HMVEC-L treated with exogenous MK protein (100 ng/ml) and heparin (20 μg/ml). Lower panels: For PKC inhibition, BIS (5 μM) was added 1 hour before a 36-hour treatment with rh-MK plus heparin. Western blot data are shown. (**B**) The data in **A** were quantified using densitometry and are presented as mean and SD (n = 3). $^{*}P < 0.05$ and $^{**}P < 0.01$ versus 0 hours. (**C**) Conversion from Ang I to Ang II by the cells treated with MK. HMVEC-L cells were treated with exogenous MK protein (100 ng/ml) and heparin (20 μg/ml) or heparin (20 μg/ml) for 36 hours. Ang I (500 pM) was then added to the medium and incubated for the indicated times (n = 5). (**D**) Phospho-PKC expression in HMVEC-L treated with exogenous MK protein (100 ng/ml) and heparin (20 μg/ml). Western blot data are shown. (**E**) The data in **D** (left panel) were quantified using densitometry and are presented as mean and SD (n = 3). $^{*}P < 0.05$ and $^{**}P < 0.01$ versus 0 hours. (**F**) Representative data from Western blotting for phospho-PKC expression in the lung. The intensity of phospho-PKC bands on Western blotting was normalized to that of β-actin (n = 5). $^{\S}P < 0.05$ versus sham *Mdk*$^{+/+}$. Western blotting results are not shown. $^{\dagger}P < 0.01$; $^{\ddagger}P < 0.05$.

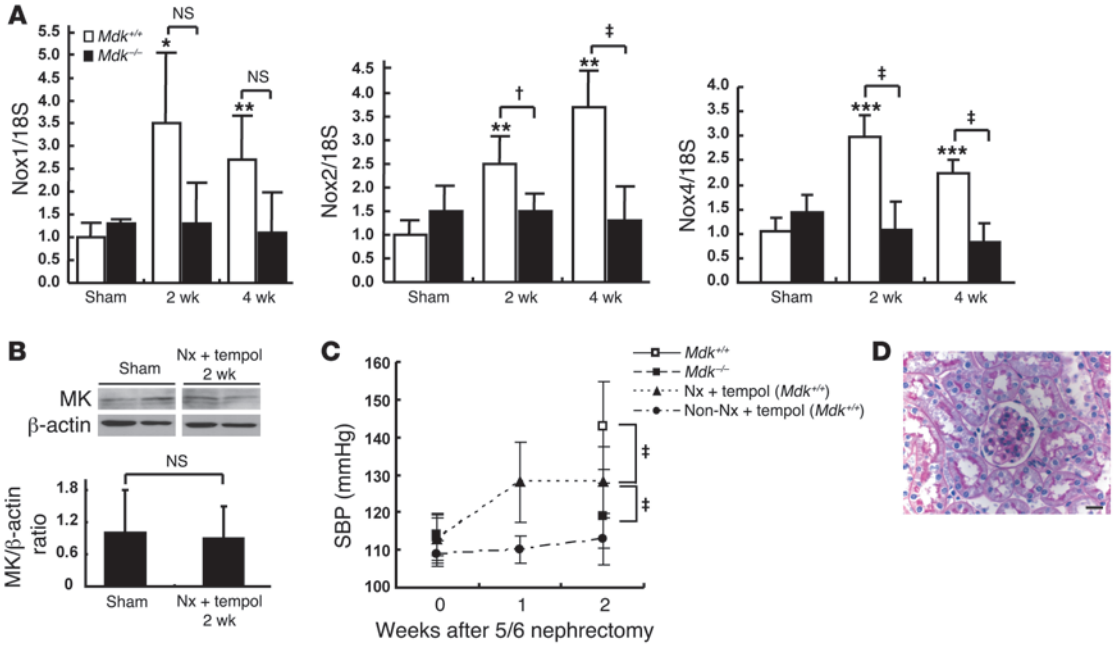

Figure 6

The mechanism of MK induction in the lung. (**A**) Time course of Nox1, -2, and -4 expression in the lung after 5/6 nephrectomy. Expression of Nox1, -2, and -4 mRNA was determined by real-time PCR. Data are presented as mean and SD ($Mdk^{+/+}$: sham, $n = 5$; 2 weeks, $n = 5$; 4 weeks, $n = 3$; $Mdk^{-/-}$: sham, $n = 3$; 2 weeks, $n = 3$; 4 weeks, $n = 3$). $^{*}P < 0.05$, $^{**}P < 0.01$, and $^{***}P < 0.001$ versus sham $Mdk^{+/+}$. (**B**) Effect of tempol on MK expression in the lung. Tempol mixed in drinking water was administered to $Mdk^{+/+}$ mice after 5/6 nephrectomy. MK protein expression was determined by Western blotting (upper panel). The intensity of MK bands on Western blotting was normalized to that of β-actin (lower panel). Data are presented as mean and SD ($n = 5$). (**C**) Effect of tempol on blood pressure after 5/6 nephrectomy. SBP was measured by the tail-cuff method. Data are presented as mean and SD ($n = 6$). (**D**) Effect of tempol on renal damage. PAS staining of a kidney specimen 2 weeks after 5/6 nephrectomy in $Mdk^{+/+}$ mice that received tempol treatment. The tubulointerstitial damage was slight compared with that in the mice without tempol treatment (Figure 1C). Scale bar: 20 μm. $^{\dagger}P < 0.05$; $^{\ddagger}P < 0.01$.

addition, we found a significant elevation of macrophage infiltration into the kidney in wild-type mice compared with $Mdk^{-/-}$ mice in the present study. This finding is consistent with our previous report showing MK-mediated macrophage recruitment in neointima formation (41). Therefore, MK-mediated inflammation in the kidney may contribute to the renal damage after 5/6 nephrectomy (Figure 7). On the other hand, in the context of inflammation and hypertension, it is important to note that inflammatory cell infiltration into the kidney does not always induce hypertension (42, 43). Furthermore, the local RAS in organs other than the lung was not activated in the present study. Thus, the relationship between intrarenal inflammation and hypertension after 5/6 nephrectomy remains to be verified.

Methods

Animals and experimental design. Mice deficient in *Mdk* were generated as described previously (44). After backcrossing of $Mdk^{+/-}$ mice for 14 generations with 129/Sv mice, $Mdk^{+/-}$ mice were mated with each other to generate $Mdk^{+/+}$ and $Mdk^{-/-}$ mice, which were used in this study. Experiments were performed on 8- to 12-week-old female mice weighing 20–25 g that were housed under controlled environmental conditions and maintained with standard food and water. Animal care and experimental procedures were approved by the Animal Experimentation Committee of the Nagoya University Graduate School of Medicine and were conducted according to the Nagoya University Regulations for Experiments. Renal ablation was performed as described previously. Briefly, mice were anesthetized by diethyl ether. The flank region was shaved, and the animals were placed on a heating pad to maintain a constant body temperature (37°C). Under anesthesia, right flank incisions were made, and the right kidney was removed. Seven days later, mice were anesthetized as above, and two-thirds of the mass of the left kidneys was ablated ($Mdk^{+/+}$: 2 weeks, $n = 13$; 4 weeks, $n = 13$; 8 weeks, $n = 8$; $Mdk^{-/-}$: 2 weeks, $n = 10$; 4 weeks, $n = 10$; 8 weeks, $n = 4$). After the renal ablation, the flanks were closed in 2 layers with 5-0 silk sutures. The animals received 100 ml/kg warm saline instilled into the peritoneal cavity during the procedure and were allowed to recover with free access to food and water. In the control mice, a sham operation was performed ($Mdk^{+/+}$, $n = 11$; $Mdk^{-/-}$, $n = 8$).

Drug treatment model. In the drug treatment studies, $Mdk^{+/+}$ mice were randomly assigned to receive one of the following 5 treatments after 5/6 nephrectomy and were orally treated daily starting from 24 hours after 5/6 nephrectomy: vasodilator (hydralazine hydrochloride; Novartis) at a dose of 10 mg/kg/d (group 1, $n = 3$); ACE inhibitor (temocapril; Daiichi Sankyo Co.) at a dose of 3 mg/kg/d (group 2, $n = 3$); angiotensin receptor blocker (olmesartan; Daiichi Sankyo Co.) at a dose of 3 mg/kg/d (group 3, $n = 3$); antioxidative reagent (tempol; Alexis Biochemicals) at a dose of 3 mmol/l in drinking solution after 5/6 nephrectomy (group 4, $n = 6$); and sham operation (group 5, $n = 6$). Drug treatment was performed at 2 weeks after 5/6 nephrectomy. In the present study, we determined the dosage according to previous reports (45–47). Blood pressure was measured by the tail-cuff method at 2 weeks, as described below under *Blood pressure monitoring*. Mice were sacrificed at 2 weeks after 5/6 nephrectomy, and blood and tissue samples were collected.

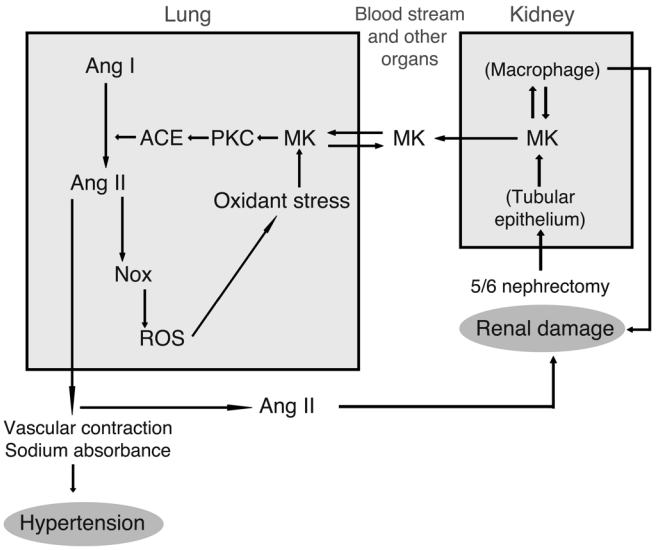

Figure 7
Schematic diagram showing the possible relationship between MK and the RAS cascade that promotes hypertension and renal damage.

MK protein and PTN protein. The recombinant human MK (rh-MK) was produced from yeast as described previously (48). In brief, human MK was produced by *Pichia pastoris* GS115 transfected with a human MK expression vector, which was constructed into pHIL-D4 (Invitrogen) (48). The MK protein was then purified by anion exchange chromatography and affinity chromatography on a heparin column. The purified human protein exhibited neurotrophic activity comparable to that of mouse MK produced in L cells (49). Recombinant human PTN was produced as previously described (50).

rh-MK and -PTN treatment model. In the pump study, MK protein in saline (1.6 mg/ml) (n = 5), PTN in saline (1.6 mg/ml; n = 5), or saline alone (n = 5) was infused using an osmotic pump (ALZA Corp.) into *Mdk*$^{-/-}$ mice after 5/6 nephrectomy. The pumps continuously infused a total of 100 μl over 14 days. The pumps were implanted under the dorsal skin the next day after 5/6 nephrectomy. Blood pressure was measured by the indirect tail-cuff technique at 0 and 2 weeks after 5/6 nephrectomy. Mice were sacrificed at 2 weeks after 5/6 nephrectomy, and blood and tissue samples were collected.

Blood pressure monitoring. Blood pressure was measured in restrained, conscious mice by the indirect tail-cuff technique under unstressed conditions (BP-98A; Softron) at 0, 2, 4, 6, and 8 weeks after 5/6 nephrectomy (51). Before measurement, the mice were warmed with a heating pad for 5 minutes. A total of 7–10 readings were taken for each mouse, at 1- to 2-minute intervals.

Sample collection. Mice were sacrificed at 2, 4, and 8 weeks after 5/6 nephrectomy. The remnant kidney, lung, brain, heart, and liver were removed rapidly, snap-frozen in liquid nitrogen, and stored at –80°C until examinations were performed. Each tissue was processed for histology, protein extraction, and RNA extraction. Blood samples were collected into chilled tubes for measurement of renal function parameters and into chilled tubes containing EDTA for Ang II measurements. Serum and plasma were separated by centrifugation (500 *g* for 10 minutes) and stored at –80°C until measurement were performed. Serum creatinine, blood urea nitrogen (*Mdk*$^{+/+}$: sham, n = 6; 2 weeks, n = 10; 4 weeks, n = 9; 8 weeks, n = 8; *Mdk*$^{-/-}$: sham, n = 7; 2 weeks, n = 7; 4 weeks, n = 6; 8 weeks, n = 4), and Ang II concentrations (*Mdk*$^{+/+}$: sham, n = 6; 2 weeks, n = 6; 4 weeks, n = 8; *Mdk*$^{-/-}$: sham, n = 6; 2 weeks, n = 7; 4 weeks, n = 5) were measured by Mitsubishi BCL.

ACE activity assay. Lung ACE activity was measured in a fluorescence assay using a commercial ACE activity assay kit (Life Laboratory Company, Yamagata, Japan). Isolated lung tissue (*Mdk*$^{+/+}$: sham, n = 5; 2 weeks, n = 5; 4 weeks, n = 5; *Mdk*$^{-/-}$: sham, n = 5; 2 weeks, n = 5; 4 weeks, n = 4) was homogenized in an assay buffer and then clarified by centrifugation at 10,000 *g* for 15 minutes at 4.0°C. ACE activity against a synthetic substrate (benzyloxycarbonyl-phenyl alanyl-leucine) was determined using a colorimetric method. The product was measured fluorometrically at 355-nm excitation and 460-nm emission with a fluoro-colorimeter, as follows. For the assay, tissue samples were standardized to 1 μg protein/ml. Results were calculated as mU/mg protein. All data are reported as mean ± SD. The measurements were performed in duplicate.

Histology and immunohistochemistry. The removed kidneys and lungs were fixed in 10% buffered formalin, embedded in paraffin, and then cut into 4-μm sections. The sections were stained with H&E, PAS, and Masson's trichrome. Another tissue sample was embedded in OCT compound (Sakura Finetek) and frozen in liquid nitrogen for immunostaining. Sections were cut to a thickness of 3 μm with a cryostat and fixed in acetone. High-power fields were used to examine the sections for evidence of focal sclerosis (52, 53). Glomerular sclerosis was assessed by semiquantitative score (grades 0 to +4) using the method of Raij et al. (54): grade 0, no sclerosis of glomeruli; grade 1, sclerosis of up to 25% of glomerulus; grade 2, sclerosis of 25%–50% of glomerulus; grade 3, sclerosis of 50%–75% of glomerulus; grade 4, sclerosis of 75%–100% of glomerulus. At least 50 glomeruli were evaluated under ×400 magnification and results averaged for each kidney (*Mdk*$^{+/+}$: 2 weeks, n = 5; 4 weeks, n = 4; 8 weeks, n = 4; *Mdk*$^{-/-}$: 2 weeks, n = 4; 4 weeks, n = 3; 8 weeks, n = 3). Immunostaining for ACE and MK was performed on buffered formalin–fixed tissues. Sections were deparaffinized, rehydrated, incubated in 3% hydrogen peroxide in methanol to block endogenous peroxidase, and washed in 10% normal goat serum (Dako) in PBS to block nonspecific binding. Subsequently, sections were incubated with mouse anti-ACE monoclonal antibody (dilution, 1:400; Chemicon International, Millipore) or anti-MK monoclonal antibody (dilution, 1:100) overnight at 4°C as described previously (22), followed by a conjugate of polyclonal goat anti-mouse IgG antibody and HRP-labeled polymer (Histofine Simple Stain; Nichirei) for 1 hour at room temperature as a secondary antibody. The staining was visualized with 3-3′ diaminobenzidine (Nichirei) to produce a brown color. The sections were covered with 90% glycerol containing *p*-phenylenediamine and were examined by electron microscopy (H-7100; Hitachi). For double immunofluorescence staining of MK and thrombomodulin as a marker of the vascular endothelium, the cryosections of lungs were first incubated with chicken anti–human MK (dilution, 1:200) and then with rabbit anti–rat thrombomodulin (dilution, 1:1,000) (55), followed by incubation with FITC-labeled rabbit anti-chicken IgG (dilution, 1:160) and rhodamine-labeled goat anti-rabbit IgG (dilution, 1:320) as secondary antibodies. For immunofluorescence staining of macrophages and neutrophils, the cryosections of lungs or kidneys were first incubated with rat anti–mouse F4/80 antibodies (MCA497F; dilution, 1:50; AbD Serotec) or rat anti-mouse neutrophils (MCA771G; dilution, 1:200; AbD Serotec), followed by incubation with FITC-labeled goat anti-rat IgG F(ab)′ 2 (dilution, 1:160) or FITC-labeled rabbit anti-rat IgG (dilution, 1:160) as secondary antibodies. The lung and kidney section from each mouse was viewed under ×400 magnification, and then macrophages or neutrophils were counted from 10 fields and averaged. Values are mean ± SD.

HMVEC-L culture and treatments. HMVEC-L were used for the in vitro assay because they have previously been shown to express ACE (56). HMVEC-L (Takara Bio Inc.) were cultivated in EGM-2MV BulletKit medium (Takara Bio Inc.) at 37°C in 5% CO_2. HMVEC-L were grown as a monolayer in tissue culture plates coated with type I collagen. When the cells reached 70%–80% confluence, they were passaged with trypsin (0.025%)/EDTA (0.01%) and used within 4 passages, as recommended by the supplier. After reaching

confluence, HMVEC-L were washed with PBS and cultured for 24 hours in essential basal medium containing 0.5% FBS. These cells were exposed to 100 ng/ml recombinant human MK (rh-MK) plus 20 μg/ml heparin or 50 ng/ml PMA (Sigma-Aldrich) in essential basal medium containing 0.5% FBS. PMA and the PKC inhibitor stock solutions were made in dimethyl sulfoxide. For PKC inhibition, BIS (Calbiochem) was added 1 hour before treatment with rh-MK plus heparin or PMA. Protein was extracted from HMVEC-L at the indicated time points after treatment. Cells were then lysed in RIPA buffer (50 mmol/l Tris-HCl, 150 mmol/l NaCl, 1% Nonidet P-40, 1% deoxycholic acid, and 0.05% sodium dodecyl sulfate) containing 0.25 mmol/l phenylmethylsulfonyl fluoride, kept on ice for 40 minutes, and then centrifuged at 15,000 *g* for 10 minutes at 4°C. The supernatants were then subjected to SDS-PAGE and Western blotting.

Ang II concentration in HMVEC-L. After reaching confluence, HMVEC-L were washed with PBS and cultured for 24 hours in essential basal medium containing 0.5% FBS. These cells were exposed to 100 ng/ml rh-MK plus 20 μg/ml heparin or 20 μg/ml heparin alone in essential basal medium containing 0.5% FBS for 36 hours. After stimulation, HMVEC-L were washed with PBS and exposed to 500 pM Ang I (Sigma-Aldrich) for 10 and 25 minutes. Supernatants were collected into chilled tubes, and then the Ang II concentration was measured as previously described (57).

Western blot analysis. Mouse kidney, lung, brain, heart, and liver tissues were snap-frozen in liquid nitrogen for protein isolation. Western blot analysis was performed as described previously (58). The blots were subsequently incubated with goat anti–human MK antibody (dilution, 1:1,000), monoclonal anti–β-actin antibody (dilution, 1:1,000; Sigma-Aldrich), mouse anti-ACE monoclonal antibody (dilution, 1:1,000; Chemicon International, Millipore), or rabbit anti–phospho-PKC antibody (dilution, 1:1,000; Cell Signaling Technology), followed by incubation with peroxidase-conjugated goat IgG, mouse IgG, or rabbit IgG (dilution, 1:5,000; Jackson Immunoresearch Laboratories Inc.). Western blot analysis of liver ANG was performed using the ANG-specific polyclonal antibody as described previously (59). Proteins were visualized with an enhanced chemiluminescence detection system (Amersham Pharmacia, GE Healthcare). The density of each band was measured using the public domain NIH Image program (http://rsb.info.nih.gov/nih-image/).

RNA preparation from mouse kidney and lung. Mouse kidney and lung tissues (15 mg) were immersed in RNA*later* (Ambion, Applied Biosystems) for 1 day. The mixture was ground for 2 minutes with 5-mm tungsten carbide beads at a frequency of 20–25 Hz using a mixer-mill grinder according to the manufacturer's instructions (Tissuelyser; QIAGEN). The ground solution was then centrifuged for 3 minutes at 10,000 *g* to compact the debris, and the supernatant was treated according to the manufacturer's instructions. Total RNA was extracted using an RNeasy Mini Kit (QIAGEN). RNA concentrations were estimated using a spectrophotometer (Ultrospec 3300 pro; Amersham Biosciences, GE Healthcare).

Real-time PCR. First-strand cDNA was synthesized using the QuantiTect Reverse Transcription Kit (QIAGEN) according to the manufacturer's instructions. One microgram of total RNA was then reverse transcribed. To validate changes in gene expression, we performed real-time PCR analysis with an Applied Biosystems Prism 7500HT Sequence Detection System using TaqMan Gene Expression Assays according to the manufacturer's specifications (Applied Biosystems). Two microliters of cDNA samples was used for the PCR reaction. The TaqMan probes and primers were as follows. For mouse MK: forward, 5′-CAAGGGACCCTGAAGAAGGC-3′, and reverse, 5′-CTTTGGTCTTTGACTTGCTCTTGG-3′; for ANG: forward, 5′-CTCGAACTCAAAGCAGGAGAGG-3′, and reverse, 5′-CGTAGATGGCGAACAGGAAGG-3′; for renin: 5′-TTGTTGCTCTGGAGTCCTTGC-3′, and reverse, 5′-CAGGATTTCCCGGACAGAAGG-3′; for ACE: forward, 5′-ACCCAACCTCGATGTCACCA-3′, and reverse, 5′-GCGAGGTGAAGAATTCCTCTGA-3′; for Nox1: forward, 5′-TTGGCACAGTCAGTGAGGATG-3′, and reverse, 5′-AGATTTCAAGATGGAAGCAAAGGG-3′; for Nox2: forward, 5′-ACTTTCCATAAGATGGTAGCTTGG-3′, and reverse, 5′-GCATTCACACACCACTCAACG-3′; and for Nox4: forward, 5′-ACCAGAATGAGGATCCCAGAAAG-3′, and reverse, 5′-GTAGAAGCTGTAACCATGAGGAAC-3′. 18S ribosomal RNA (assay identification number 4326317E), which was used as an endogenous control, was as assay-on-demand gene expression product (Applied Biosystems). The thermal cycler conditions were as follows: hold for 10 minutes at 95°C, followed by 2-step PCR consisting of 40 cycles at 95°C for 15 seconds and 60°C for 1 minute. The relative quantification of all targets was carried out using the comparative cycle threshold method (60). The levels of gene expression were standardized with those of the 18S ribosomal RNA.

Statistics. Results are expressed as mean ± SD. Statistical difference was assessed by a single-factor variance (ANOVA) followed by a 2-tailed unpaired *t* test, as appropriate. *P* values less than 0.05 were considered significant.

Acknowledgments

We thank Norihiko Suzuki, Naoko Asano, Yuriko Sawa, and Kayoko Miyata for their excellent technical assistance. This work was supported in part by the 21st Century COE Program and Global COE program, Ministry of Education, Culture, Sports, Science, and Technology, Japan.

Received for publication August 25, 2008, and accepted in revised form March 25, 2009.

Address correspondence to: Kenji Kadomatsu, Department of Biochemistry, Nagoya University Graduate School of Medicine, 65 Tsurumai-cho, Showa-ku, Nagoya 466-8550, Japan. Phone: 81-52-744-2059; Fax: 81-52-744-2065; E-mail: kkadoma@med.nagoya-u.ac.jp.

1. Atlas, S.A. 2007. The renin-angiotensin aldosterone system: pathophysiological role and pharmacologic inhibition. *J. Manag. Care Pharm.* **13**:9–20.
2. Kobori, H., Nangaku, M., Navar, L.G., and Nishiyama, A. 2007. The intrarenal renin-angiotensin system: from physiology to the pathobiology of hypertension and kidney disease. *Pharmacol. Rev.* **59**:251–287.
3. Ruster, C., and Wolf, G. 2006. Renin-angiotensin-aldosterone system and progression of renal disease. *J. Am. Soc. Nephrol.* **17**:2985–2991.
4. Skeggs, L.T., Jr., Kahn, J.R., Lentz, K., and Shumway, N.P. 1957. The preparation, purification, and amino acid sequence of a polypeptide renin substrate. *J. Exp. Med.* **106**:439–453.
5. Dzau, V.J. 1988. Tissue renin-angiotensin system: physiologic and pharmacologic implications. Introduction. *Circulation.* **77**:I1–I3.
6. Sayed-Tabatabaei, F.A., Oostra, B.A., Isaacs, A., van Duijn, C.M., and Witteman, J.C. 2006. ACE polymorphisms. *Circ. Res.* **98**:1123–1133.
7. Remuzzi, G., Perico, N., Macia, M., and Ruggenenti, P. 2005. The role of renin-angiotensin-aldosterone system in the progression of chronic kidney disease. *Kidney Int. Suppl.* S57–S65.
8. Kadomatsu, K., and Muramatsu, T. 2004. Midkine and pleiotrophin in neural development and cancer. *Cancer Lett.* **204**:127–143.
9. Sato, W., et al. 2005. Midkine antisense oligodeoxyribonucleotide inhibits renal damage induced by ischemic reperfusion. *Kidney Int.* **67**:1330–1339.
10. Kosugi, T., et al. 2006. Growth factor midkine is involved in the pathogenesis of diabetic nephropathy. *Am. J. Pathol.* **168**:9–19.
11. Ezquerra, L., Herradon, G., Nguyen, T., Silos-Santiago, I., and Deuel, T.F. 2005. Midkine, a newly discovered regulator of the renin-angiotensin pathway in mouse aorta: significance of the pleiotrophin/midkine developmental gene family in angiotensin II signaling. *Biochem. Biophys. Res. Commun.* **333**:636–643.
12. Werner, C., et al. 2008. RAS blockade with ARB and ACE inhibitors: current perspective on rationale and patient selection. *Clin. Res. Cardiol.* **97**:418–431.
13. Wuhl, E., and Schaefer, F. 2008. Therapeutic strategies to slow chronic kidney disease progression. *Pediatr. Nephrol.* **23**:705–716.
14. Ferrari, P. 2007. Prescribing angiotensin-converting enzyme inhibitors and angiotensin receptor blockers in chronic kidney disease. *Nephrology (Carlton).* **12**:81–89.

15. Olson, J.L., Hostetter, T.H., Rennke, H.G., Brenner, B.M., and Venkatachalam, M.A. 1982. Altered glomerular permselectivity and progressive sclerosis following extreme ablation of renal mass. *Kidney Int.* **22**:112–126.
16. Hostetter, T.H., Olson, J.L., Rennke, H.G., Venkatachalam, M.A., and Brenner, B.M. 1981. Hyperfiltration in remnant nephrons: a potentially adverse response to renal ablation. *Am. J. Physiol.* **241**:F85–F93.
17. Dikow, R., et al. 2004. Increased infarct size in uremic rats: reduced ischemia tolerance? *J. Am. Soc. Nephrol.* **15**:1530–1536.
18. van Dokkum, R.P., et al. 2004. Myocardial infarction enhances progressive renal damage in an experimental model for cardio-renal interaction. *J. Am. Soc. Nephrol.* **15**:3103–3110.
19. Pupilli, C., Chevalier, R.L., Carey, R.M., and Gomez, R.A. 1992. Distribution and content of renin and renin mRNA in remnant kidney of adult rat. *Am. J. Physiol.* **263**:F731–F738.
20. Nishimura, M., Takahashi, H., and Yoshimura, M. 2007. Upregulation of the brain renin-angiotensin system in rats with chronic renal failure. *Acta Physiol. (Oxf.).* **189**:369–377.
21. Riordan, J.F. 2003. Angiotensin-I-converting enzyme and its relatives. *Genome Biol.* **4**:225.
22. Sato, W., et al. 2001. Midkine is involved in neutrophil infiltration into the tubulointerstitium in ischemic renal injury. *J. Immunol.* **167**:3463–3469.
23. Narita, H., Chen, S., Komori, K., and Kadomatsu, K. 2008. Midkine is expressed by infiltrating macrophages in in-stent restenosis in hypercholesterolemic rabbits. *J. Vasc. Surg.* **47**:1322–1329.
24. Inoh, K., Muramatsu, H., Ochiai, K., Torii, S., and Muramatsu, T. 2004. Midkine, a heparin-binding cytokine, plays key roles in intraperitoneal adhesions. *Biochem. Biophys. Res. Commun.* **317**:108–113.
25. Villard, E., Alonso, A., Agrapart, M., Challah, M., and Soubrier, F. 1998. Induction of angiotensin I-converting enzyme transcription by a protein kinase C-dependent mechanism in human endothelial cells. *J. Biol. Chem.* **273**:25191–25197.
26. Touyz, R.M. 2003. Reactive oxygen species in vascular biology: role in arterial hypertension. *Expert Rev. Cardiovasc. Ther.* **1**:91–106.
27. Vaziri, N.D., and Rodriguez-Iturbe, B. 2006. Mechanisms of disease: oxidative stress and inflammation in the pathogenesis of hypertension. *Nat. Clin. Pract. Nephrol.* **2**:582–593.
28. Hoke, T.S., et al. 2007. Acute renal failure after bilateral nephrectomy is associated with cytokine-mediated pulmonary injury. *J. Am. Soc. Nephrol.* **18**:155–164.
29. Kelly, K.J. 2003. Distant effects of experimental renal ischemia/reperfusion injury. *J. Am. Soc. Nephrol.* **14**:1549–1558.
30. Anavekar, N.S., et al. 2004. Relation between renal dysfunction and cardiovascular outcomes after myocardial infarction. *N. Engl. J. Med.* **351**:1285–1295.
31. Amann, K., Wanner, C., and Ritz, E. 2006. Cross-talk between the kidney and the cardiovascular system. *J. Am. Soc. Nephrol.* **17**:2112–2119.
32. Kuczera, M., et al. 1991. Local angiotensin formation in hindlimbs of uremic hypertensive and renovascular hypertensive rats. *J. Hypertens.* **9**:41–48.
33. Kidney Disease Outcomes Quality Initiative (K/DOQI). 2004. K/DOQI clinical practice guidelines on hypertension and antihypertensive agents in chronic kidney disease. *Am. J. Kidney Dis.* **43**(5 Suppl. 1):S1–S290.
34. Iannone, A., Bini, A., Swartz, H.M., Tomasi, A., and Vannini, V. 1989. Metabolism in rat liver microsomes of the nitroxide spin probe tempol. *Biochem. Pharmacol.* **38**:2581–2586.
35. Schnackenberg, C.G., and Wilcox, C.S. 1999. Two-week administration of tempol attenuates both hypertension and renal excretion of 8-Iso prostaglandin f2alpha. *Hypertension.* **33**:424–428.
36. Johnson, F., and Giulivi, C. 2005. Superoxide dismutases and their impact upon human health. *Mol. Aspects Med.* **26**:340–352.
37. Mollnau, H., et al. 2002. Effects of angiotensin II infusion on the expression and function of NAD(P)H oxidase and components of nitric oxide/cGMP signaling. *Circ. Res.* **90**:E58–E65.
38. Liao, T.D., et al. 2008. Role of inflammation in the development of renal damage and dysfunction in angiotensin II-induced hypertension. *Hypertension.* **52**:256–263.
39. Kobori, H., Prieto-Carrasquero, M.C., Ozawa, Y., and Navar, L.G. 2004. AT1 receptor mediated augmentation of intrarenal angiotensinogen in angiotensin II-dependent hypertension. *Hypertension.* **43**:1126–1132.
40. Graciano, M.L., et al. 2008. Purinergic receptors contribute to early mesangial cell transformation and renal vessel hypertrophy during angiotensin II-induced hypertension. *Am. J. Physiol. Renal Physiol.* **294**:F161–F169.
41. Horiba, M., et al. 2000. Neointima formation in a restenosis model is suppressed in midkine-deficient mice. *J. Clin. Invest.* **105**:489–495.
42. Tu, X., et al. 2008. Anti-inflammatory renoprotective effect of clopidogrel and irbesartan in chronic renal injury. *J. Am. Soc. Nephrol.* **19**:77–83.
43. Usui, H.K., et al. 2007. Macrophage scavenger receptor-a-deficient mice are resistant against diabetic nephropathy through amelioration of microinflammation. *Diabetes* **56**:363–372.
44. Nakamura, E., et al. 1998. Disruption of the midkine gene (Mdk) resulted in altered expression of a calcium binding protein in the hippocampus of infant mice and their abnormal behaviour. *Genes Cells.* **3**:811–822.
45. Sada, T., Koike, H., Nishino, H., and Oizumi, K. 1989. Chronic inhibition of angiotensin converting enzyme decreases Ca2+-dependent tone of aorta in hypertensive rats. *Hypertension.* **13**:582–588.
46. Yoshida, K., Xu, H.L., Kawamura, T., Ji, L., and Kohzuki, M. 2002. Chronic angiotensin-converting enzyme inhibition and angiotensin II antagonism in rats with chronic renal failure. *J. Cardiovasc. Pharmacol.* **40**:533–542.
47. Nishiyama, A., et al. 2004. Possible contributions of reactive oxygen species and mitogen-activated protein kinase to renal injury in aldosterone/salt-induced hypertensive rats. *Hypertension.* **43**:841–848.
48. Ikematsu, S., et al. 2000. Serum midkine levels are increased in patients with various types of carcinomas. *Br. J. Cancer.* **83**:701–706.
49. Muramatsu, H., and Muramatsu, T. 1991. Purification of recombinant midkine and examination of its biological activities: functional comparison of new heparin binding factors. *Biochem. Biophys. Res. Commun.* **177**:652–658.
50. Murasugi, A., Kido, I., Kumai, H., and Asami, Y. 2003. Efficient production of recombinant human pleiotrophin in yeast, Pichia pastoris. *Biosci. Biotechnol. Biochem.* **67**:2288–2290.
51. Pfeffer, J.M., Pfeffer, M.A., and Frohlich, E.D. 1971. Validity of an indirect tail-cuff method for determining systolic arterial pressure in unanesthetized normotensive and spontaneously hypertensive rats. *J. Lab. Clin. Med.* **78**:957–962.
52. Kohzuki, M., et al. 1995. Kinin and angiotensin II receptor antagonists in rats with chronic renal failure: chronic effects on cardio- and renoprotection of angiotensin converting enzyme inhibitors. *J. Hypertens.* **13**:1785–1790.
53. Saito, T., et al. 1990. Progression of experimental focal glomerulosclerosis in the spontaneously hypertensive rat. *J. Lab. Clin. Med.* **115**:165–173.
54. Raij, L., Azar, S., and Keane, W. 1984. Mesangial immune injury, hypertension, and progressive glomerular damage in Dahl rats. *Kidney Int.* **26**:137–143.
55. Yuzawa, Y., et al. 1993. Antibody-mediated redistribution and shedding of endothelial antigens in the rabbit. *J. Immunol.* **150**:5633–5646.
56. Shen, J., Ham, R.G., and Karmiol, S. 1995. Expression of adhesion molecules in cultured human pulmonary microvascular endothelial cells. *Microvasc. Res.* **50**:360–372.
57. Nishiyama, A., Seth, D.M., and Navar, L.G. 2002. Renal interstitial fluid concentrations of angiotensins I and II in anesthetized rats. *Hypertension.* **39**:129–134.
58. Kadomatsu, K., et al. 1997. Midkine induces the transformation of NIH3T3 cells. *Br. J. Cancer.* **75**:354–359.
59. Kobori, H., Harrison-Bernard, L.M., and Navar, L.G. 2001. Expression of angiotensinogen mRNA and protein in angiotensin II-dependent hypertension. *J. Am. Soc. Nephrol.* **12**:431–439.
60. Livak, K.J., and Schmittgen, T.D. 2001. Analysis of relative gene expression data using real-time quantitative PCR and the 2(-delta delta C(T)) method. *Methods.* **25**:402–408.